Biochemical and Biophysical Research Communications 426 (2012) 165–171

Contents lists available at SciVerse ScienceDirect

Biochemical and Biophysical Research Communications

journal homepage: www.elsevier.com/locate/ybbrc

Formation of spherulitic amyloid β aggregate by anionic liposomes

Toshinori Shimanouchi [a], Naoya Shimauchi [a], Ryo Ohnishi [a], Nachi Kitaura [a], Hisashi Yagi [b], Yuji Goto [b], Hiroshi Umakoshi [a,*], Ryoichi Kuboi [a]

[a] Graduate School of Engineering Science, Osaka University, 1-3 Machikaneyama-cho, Toyonaka, Osaka 560-8531, Japan
[b] Institute for Protein Research, Osaka University, 3-2 Yamadaoka, Suita, Osaka 565-0871, Japan

ARTICLE INFO

Article history:
Received 17 July 2012
Available online 27 July 2012

Keywords:
Protein aggregation
Amyloid
Liposome
Alzheimer's disease

ABSTRACT

Alzheimer's disease is the most common form of senile dementia. This neurodegenerative disorder is characterized by an amyloid deposition in senile plaques, composed primarily of fibrils of an aggregated peptide, amyloid β (Aβ). The modeling of a senile plaque formation on a model neuronal membrane under the physiological condition is an attractive issue. In this study, we used anionic liposomes to model the senile plaque formation by Aβ. The growth behavior of amyloid Aβ fibrils was directly observed, revealing that the induction of the spherulitic Aβ aggregates could result from the growth of seeds in the presence of anionic liposomes. The seeds of Aβ fibrils strongly interacted with negatively charged liposome and the subsequent association of the seeds were induced to form the seed cluster with many growth ends, which is advantageous for the formation of spherulitic Aβ aggregates. Therefore, anionic liposomes mediated not only fibril growth but also the aggregation process. These results imply that anionic liposome membranes would affect the aggregate form of Aβ fibrils. The modeling of senile plaque reported here is considered to have great potential for study on the amyloidosis.

1. Introduction

Amyloid β protein (Aβ) is a soluble protein with 4.5 kDa peptide related to Alzheimer's Disease (AD) [1]. Aggregate of Aβ on neuronal cell membrane is a hallmark of AD. A recent study has demonstrated the presence of morphology of Aβ such as a fibrillar aggregate, an amorphous, a spherulitic fibrillar aggregate (spherulite). In particular, the spherulite, which is the supramolecular assemblies of Aβ fibrils, has recently become an attractive issue since it has a similar structure with that of senile plaque on neuronal cell membrane [2]. Previously, the spherulite has been reported to be induced under the higher concentration (mg/ml order) at lower pH condition [3,4] or on the surface modified with negatively charged polymers [5]. However, the morphology of amyloid Aβ fibrils of on model biomembranes has not been clarified yet under physiological conditions.

Liposome, a closed bilayer phospholipid membrane, is a useful model biomembrane system. It has been widely studied that the liposome interacts with monomeric Aβ [6–9], which is advantageous for condensation of Aβ on liposome membranes. The structure of amyloid formed on anionic liposome membranes is different from that formed in a bulk aqueous solution [10] although they did not mention to the morphology of Aβ amyloid fibrils on the liposome membranes.

In this study, the growth behavior of the seeds of Aβ(1–40) fibrils was investigated in the presence of the negatively charged liposomes. The fibril growth was then analyzed kinetically in terms of the interaction between Aβ(1–40) and liposomes. Finally we discussed the mechanism on the formation of spherulite of Aβ(1–40) fibrils mediated by the liposome membrane.

2. Materials and methods

2.1. Materials

1,2-Dimyristoyl-*sn*-glycero-3-phosphocholine (DMPC), 1,2-dimyristoyl-*sn*-glycero-3-phospho-rac-(1-glycerol) sodium salt (DMPG), 1,2-dimyristoly-phosphatidic acid (DMPA), and 1,2-dimyristoly-phosphatidyl serine (DMPS) were obtained from Avanti Polar Lipids (Alabaster, AL). Aβ(1–40) peptide was purchased from the Peptide Institute (Osaka, Japan). Thioflavin T for monitoring of fibrillization was obtained from Dojindo (Kumamoto, Japan). Other regents used were of analytical grade.

2.2. Liposome preparation

Liposomes composed of DMPC and DMPG and their mixture were prepared and characterized as described elsewhere. In brief, lipids were mixed in a chloroform/methanol mixture. The solvent was removed by evaporation in a rotary evaporator. The residual lipid film, after drying under vacuum overnight, was hydrated with

* Corresponding author. Fax: +81 (06) 6850 6286.
E-mail address: umakoshi@cheng.es.osaka-u.ac.jp (H. Umakoshi).

0006-291X/$ - see front matter © 2012 Elsevier Inc. All rights reserved.
http://dx.doi.org/10.1016/j.bbrc.2012.07.107

buffer (50 mM Tris–HCl, 100 mM NaCl, pH 7.5) and vortex-mixed to produce multilamellar vesicles. The suspension was subjected to five cycles of freezing and thawing and then extruded through polycarbonate filters (100-nm pore size filter, 11 times) using a Liposofast extruder (Avestin, Ottawa, Canada). The same was for the preparation of DMPA and DMPS liposomes. The lipid concentration was determined in triplicate by phosphorus analysis.

2.3. Amyloid peptide

Aβ(1–40) peptide was dissolved in a 0.02% ammonia solution to 200 μM at 4 °C. Aβ(1–40) amyloid fibrils were prepared by the fibril extension method as previously described [12]. Seeds were prepared by the fragmentation of amyloid fibrils for 5 min with a TOMY UD-2000 sonicator (Osaka, Japan) equipped with a microtip. The resulting solution was centrifuged to recover seeds as a supernatant from the precipitates including the remaining fibrils and the fragmented microtip. We preliminary confirmed that the seeds obtained here promoted the elongation of Aβ(1–40). The obtained seeds were added to a monomeric Aβ(1–40) (5 or 50 μM) in 50 mM Tris buffer at pH 7.5 and 100 mM NaCl and 250 μM liposome.

2.4. Thioflavin T assay for fibril growth

All studies were performed essentially as described elsewhere [3] on Jasco FP-6500 spectrofluorometer fitted with a water-jacketed cell holder shell at 4 °C with a thermodynamically controlled water bath. Optimum Thioflavin T (ThT) fluorescence measurements of Aβ were obtained at the excitation and emission wavelengths of 446 and 490 nm, respectively, with the reaction mixture containing 5 μM ThT and 50 mM Tris buffer, pH 7.5. Fluorescence was measured for immediately after making the mixture and was averaged for the initial 5 s.

2.5. SEM observation

Aβ fibrillation was performed by mixing seed of Aβ(1–40) with monomer to incubate them for more than 24 h at 37 °C, in the presence or absence of adequate liposomes. Afterward, the suspension was mixed with chloroform and filtrated by a polycarbonate filter (2 nm in pore size) to eliminate liposome from Aβ fibrils. Furthermore, this sample was washed by distilled water 10 times for removal of salts. This membrane filter containing Aβ fibril was sputtered with Pt and observed with a scanning electron microscopy (S-3000) from the angle of 30 degrees against the surface in order to get the conformation of targets.

2.6. TEM observation

The image of Aβ fibrils was obtained by a transmission electron microscope (TEM) according to the previous method [2]. In brief, a 5-μl aliquot of diluted solution was placed on a copper grid (400-mesh) covered with a carbon-coated collodion film for 1 min and the excess sample solution was removed by blotting with filter paper. After the residual solution had dried up, the grid was negatively stained with a 2% (wt./vol) uranyl acetate solution. Again, the liquid on the grid was removed with filter paper and dried. TEM images were acquired using a JEOL JEM-1200EX transmission microscope (JEOL, Tokyo, Japan) with an acceleration voltage of 80 kV.

2.7. TIRFM observation

The fluorescence microscopic system used to observe individual amyloid fibrils was developed based on an inverted microscope (IX70; Olympus, Tokyo, Japan) as described previously [2]. The ThT molecule was excited using an argon laser (model 185F02-ADM; Spectra Physics, Mountain View, CA). The fluorescent image was filtered with a bandpass filter (D490/30 Omega Optical, Brattleboro, VT) and visualized using an image intensifier (model VS4–1845; Video Scope International, Sterling, VA) coupled with a SIT camera (C2400–08; Hamamatsu Photonics, Shizuoka, Japan). Sample solution was prepared to be the final concentrations as below: Aβ(1–40) 50 μM, seed 13 μg/ml, liposome 250 μM, and Tris buffer 50 mM. After this reaction mixture was incubated at 37 °C for 24 h, ThT was added to an aliquot of this mixture at final concentration of 5 μM. And the sample of 14 μL was used for the observation.

2.8. AFM observation

A parts of samples used in TIRFM observation were placed on the mica substrate, with a micropipette. Before drying a sample, the mica was set on the stage of AFM instrument.

2.9. Calcein leakage assay

Calcein release from liposome was evaluated according to the previous report [9]. DMPC and DMPG liposomes containing calcein (0.1 M) were prepared in a similar manner to that described above for liposomes in pure buffer solution, with the only difference being that the solution with which the lipids were hydrated was 0.1 M Tris–HCl, pH 7.5, containing 0.1 M calcein. Untrapped calcein molecules were removed from the calcein-containing vesicles by size exclusion chromatography using a Sepharose 4B column (diameter: 1 cm, length: 15 cm; applied sample volume: 0.5 ml, and 0.1 M Tris–HCl, 150 mM NaCl, pH 7.5 as elution buffer). The fluorescence intensity of the vesicles containing entrapped calcein was measured and found to be low due to self-quenching. To follow the release of entrapped calcein after peptide addition, a peptide solution was mixed with a DMPC and DMPG LUV suspension to yield 0.1 mM DMPC and DMPG lipids and 10 μM peptides. The change in fluorescence intensity due to calcein release from the vesicles was monitored with a FP-6500 fluorescence spectrometer from Nihon Bunko, Japan. Excitation and emission wavelengths were set at 490 and 520 nm, respectively. The amount of calcein released after time t was calculated according to Eq. (1)

$$\mathrm{RF}(\%) = 100(I_t - I_0)/(I_{\max} - I_0) \quad (1)$$

where RF is the fraction of calcein released, I_0, I_t and $I_{\max}$ are the fluorescence intensities measured at the beginning of the experiment, at time t, and after addition of 3% triton X-100, respectively.

2.10. CD spectroscopy

The secondary structures of Aβ(1–40) in the absence and the presence of liposomes were analyzed by using a circular dichroism spectrometer (J-720 W, JASCO, Tokyo, Japan). CD spectra were measured by using a quartz cell from 195 to 250 nm with a step interval 0.1 nm bandwidth and a scanning speed of 10 nm min^{-1}.

3. Results and discussion

3.1. Observation of amyloid in the presence of liposomes

The liposome prepared by anionic phospholipids, such as phosphatidic acid and phosphatidyl serine, have been reported to promote the fibrillation of Aβ(1–40) [11]. Another previous report indicated that the negatively charged surface is a key for the generation of spherulitic structure, which is different from the amyloid

fibril structure [5]. It is therefore expected that the negatively charged liposome may contribute to the modulation of morphology of fibrils. We observed the morphology of amyloid fibrils, in the presence of the negatively charged liposome.

The growth of seeds of Aβ(1–40) fibrils in the presence of anionic 1,2-dimirystoyl-*sn*-phosphoatidylglycerol (DMPG) liposome was first observed with a scanning electron microscopy (SEM) observation. It is noted that the SEM is useful for reproducing the huge structure including spherulitic structures as previously reported in the case of bovine insulin [3]. SEM image implies the spherulitic structure (Fig. 1A). This aggregate can be stained with a Thioflavin T (ThT) to give its fluorescence. As shown in Fig. 1B, a total internal reflection fluorescence microscopy (TIRFM) image reveals that a spherulitic structure obtained here was composed of amyloid-like structures in accordance with previous reports [2]. As another evidence, a polarized microscopy (PM) observation showed the Maltese-cross, which is a typical image of the spherulitic aggregate (Fig. 1C). The size distribution obtained from TIRFM observations indicated the spherulitic structures with $6 \sim 30$ μm (Fig. 1F). Furthermore, the microscopic structure of spherulitic structures was confirmed with a transmission electron microscopy (TEM) observation. The resulting TEM image indicated the clustered fibrils (Fig. 1D). Each fibril are straight and rigid fibrillar structure (Fig. 1E). Those finding suggested a radial type growth. Together with this, we confirmed the spectroscopic feature of the spherulitic aggregate with a circular dichroic measurement. In the case of the sample used in TIRFM observation, a typical negative Cotton effect was observed at 218 nm similar to the fibrils normally prepared (Fig. 1G), suggesting a involvement of β-sheet structure in spherulites.

Aleternatively, fibrils with typical β-sheet structure were observed in the absence of liposome and the presence of the neutral 1,2-dimirystoyl-*sn*-glycero-3-phosphocholine (DMPC) liposome, as demonstrated in Fig. 1G. Meanwhile, those fibrils were not sperulitic (Fig. 1H and I).

From those results, it is considered that DMPG liposomes could induce the spherulitic fibrillar aggregates of Aβ.

3.2. Effects of liposome composition

To characterize the effect of DMPG on the induction of spherulitic fibrillar aggregate, we examined the morphology of amyloid fi-

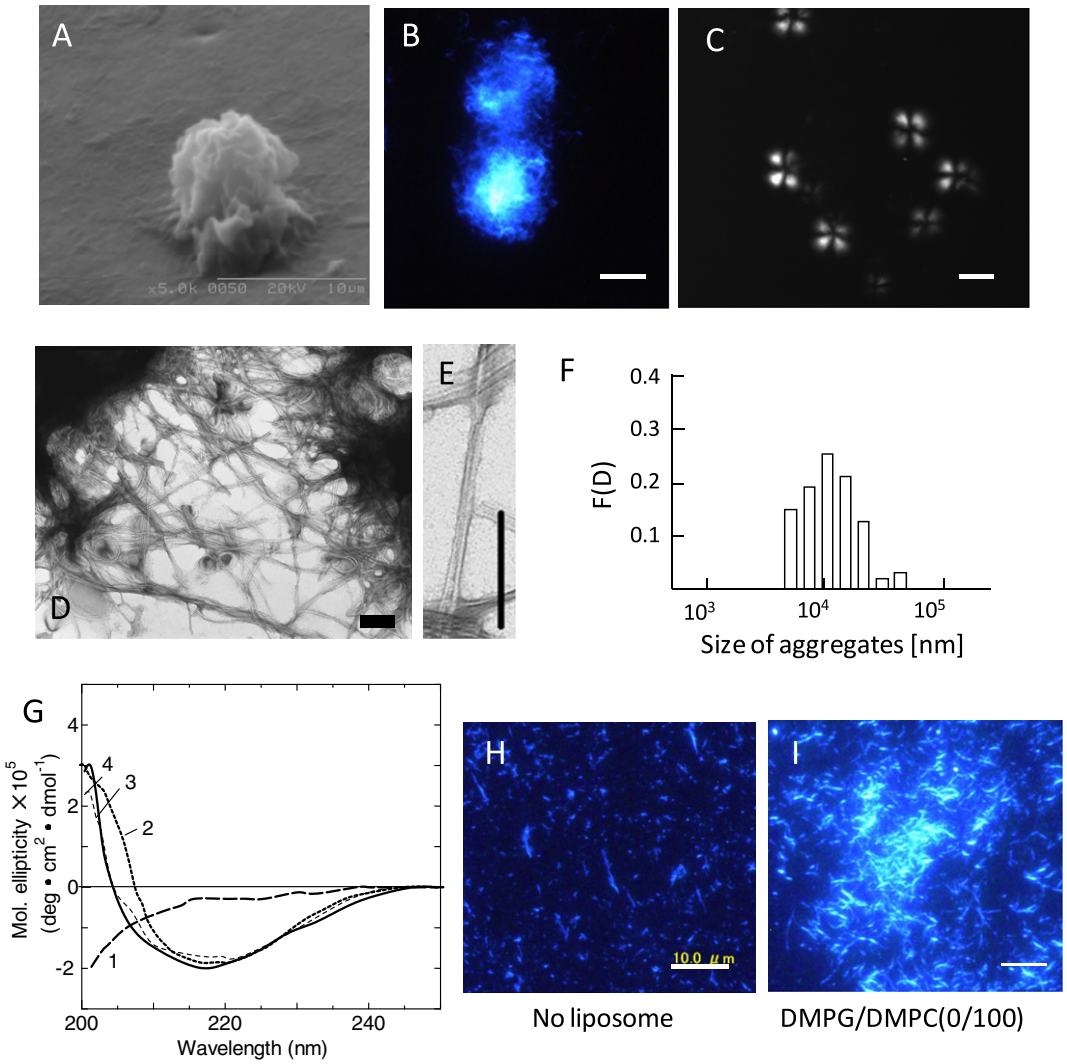

Fig. 1. Observation of the fibrils grown from the seeds of Aβ fibrils in the presence of negatively charged DMPG liposomes. (A) SEM, (B) TIRFM, (C) PM, (D) TEM, and (E) its magnified image of (D). (F) Size distribution of spherulites. F(*D*) is the fraction of spherulites with *D* in diameter. (G) CD spectra for each fibrils prepared from their seeds. 1: monomeric Aβ(1–40), 2: Aβ fibrils, 3: Aβ fibrils with DMPC, 4: Aβ fibrils with DMPG. Fibrils formed in (H) the bulk aqueous phase and in the presence of (I) uncharged DMPC. SEM image was taken at the angle of 30° from the surface. The concentration of monomeric Aβ(1–40) was 50 μM in TIRFM observation otherwise 5 μM. Bars: (white)10 μm (black) 200 nm.

brils in the case of liposome with DMPG/DMPC binary system. Below 50 mol% of DMPG, no spherulitic fibrillar aggregate was observed (Fig. 2A and B). At 50 mol% of DMPG, the incomplete spherulitic structure of amyloid was induced (Fig. 2C) although its number density was lower than that of DMPG liposome. Further increase of DMPG ratio to DMPC could resulted in a formation of complete spherulitic fibrillar aggregates (Fig. 2D and E). If DMPG liposomes were mixed with DMPC liposomes, non sperulitic fibrillar aggregates were observed together with spherulitic fibrillar aggregate (Fig. 2F). It is thus considered that the negatively charged DMPG was a key for an induction of spherulitic fibrillar aggregates. Besides, we could also observe the formation of spherulitic aggregate of Aβ(1–40) fibrils in the presence of another anionic liposomes composed of 1,2-dimirylstoyl-phospatidic acid (DMPA) (Fig. 2G) or 1,2-dimirylstoyl-phospatidylserine (DMPS) (Fig. 2H), suggesting that negatively charge of liposome membranes rather than the conformation of headgroup of lipids was a decisive factor for an induction of spherulitic fibrillar aggregates.

The aforementioned results suggested the contribution of anionic liposome membranes to the formation of spherulitic structures of fibrils.

3.3. Growth behavior of Aβ fibrils

To assess the effect of liposome against the formation process of spherulite, the growth behavior of seeds of Aβ(1–40) fibrils was examined with ThT fluorescence assay. The time-course of ThT fluorescence intensity of 5 μM Aβ(1–40) solution was monitored in the absence and the presence of liposomes (250 μM) as shown in Fig. 3A.

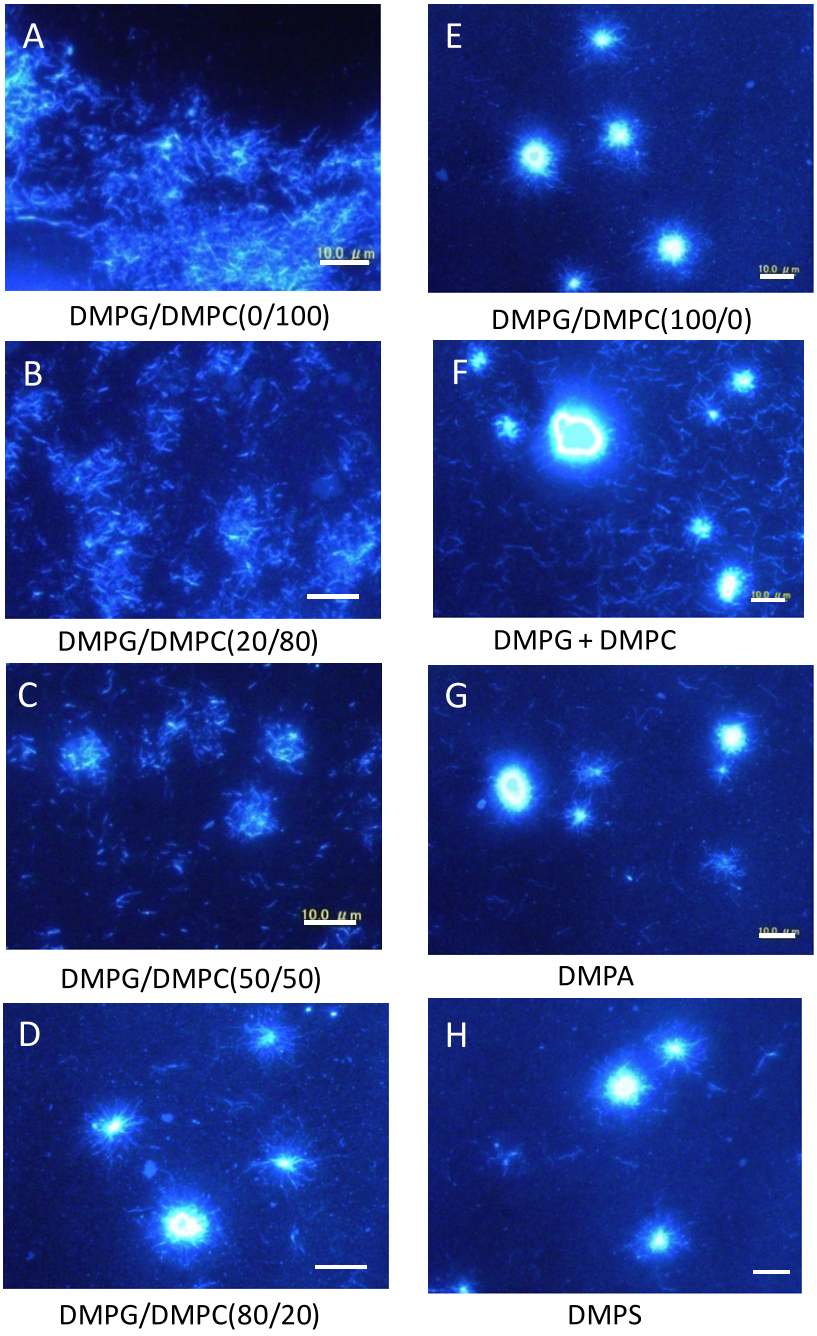

Fig. 2. Observation of the fibrils grown from the seeds of Aβ fibrils in the presence of the variety of liposomes. (A–E) DMPC/DMPG (0–100 mol%), (F) DMPG + DMPC, (G) DMPA, and (H) DMPS liposomes. Bars represent 10 μm.

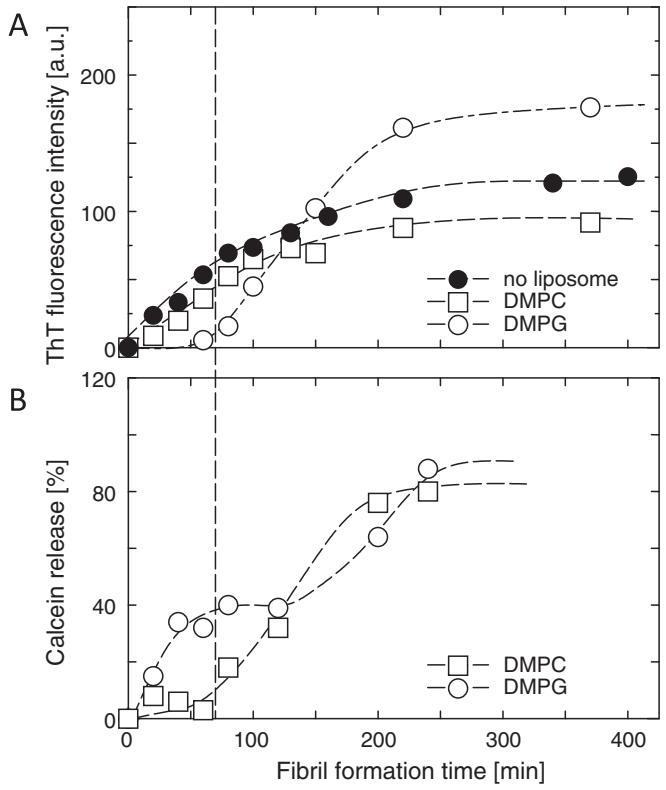

Fig. 3. (A) Time-course of ThT fluorescence intensity in the absence and the presence of liposomes. Growth of seeds in the bulk phase (closed circle), in the presence of uncharged DMPC liposome (open circle) or negatively charged DMPG liposome (open polygon). (B) Calcein release behavior from the liposome. Symbols: open circle: uncharged DMPC liposome; open polygon: negatively charged DMPG liposome. The concentration of monomeric Aβ(1–40) and lipids were 5 and 250 μM, respectively. The concentration of entrapped calcein in liposome was 100 mM. All the experiments were performed at 37 °C.

In the bulk aqueous solution, the time-course of ThT showed the first-order kinetic consistent with previous data [5,12,13]. The apparent kinetic constant, k_G, which means the elongation rate constant, was estimated to be 1.67×10^{-2} min^{-1}. The growth behavior in the presence of DMPC liposome was also similar to that in the bulk aqueous solution. The estimated k_G value was 1.81×10^{-2} min^{-1}, resulting that DMPC liposome could modulate the elongation process. The structure of the fibrils formed in the presence of liposome membranes was different from that formed in the bulk solution [10]. The growth behavior assessed by the k_G value might therefore be related to the fibril structure. On the other hand, the growth behavior in the presence of DMPG liposome differed from the above two cases. The lag-phase was observed during ~60 min of the beginning of the fibril growth. The same was true for DMPA and DMPS liposomes (data not shown). Besides, the same was also true for the formation of spherulitic fibrillar aggregates of Aβ(1–40) on the hydrophilic or negatively charged surface such as polyethyleneimine/polyvinylsulfonate membrane prepared by their layer-by-layer deposition [5].

From these observations, the initial process (lag-phase) at a beginning of 60 min might be a key process for the polymorphism of amyloid fibrils. In the following, we investigated the liposome-seed interaction.

3.4. Interaction between liposome membranes and seeds of Aβ fibrils

Liposome entrapping fluorescence probe, calcein, was mixed with Aβ seeds to investigate the interaction between liposomes and seeds. The calcein leakage from liposome, RF, was monitored since the *RF* value means the liposome-target molecule interaction due to the membrane perturbation effect [9]. The RF value for DMPG liposome at the first 60 min showed the significant leakage by seed while no leakage in the case of DMPC (Fig. 3B), strongly suggesting that the seeds interacted with DMPG liposome without the elongation of amyloid during a lag-phase observed in ThT assay. The latter phase observed in DMPG liposomes, where the RF value increased until 200 min, is corresponding to the growth phase of fibrils. In the case of DMPA or DMPS liposomes, the similar variation of RF value to Fig. 3B was observed (data not shown).

It is therefore considered that the initial stage (0 ~ 60 min) is the aggregation process of seeds induced by anionic liposomes.

3.5. Possible mechanism on liposome-mediated growth of amyloid fibrils and control of their morphology

First of all, we considered the interaction between Aβ(1–40) seeds and DMPG liposome in terms of the electrostatic interaction. Matsuzaki and coworkers (2008) have reported that the net charge of monomeric Aβ(1–40) at physiological condition was slightly negative [8] on a basis of the calculation using the pK_a value for His^{13}, His^{14}, Glu^{22} and Asp^{23} of Aβ(1–40) and Glu^{3}, Glu^{11}, His^{6}, Asp^{1}, Asp^{7} and Tyr^{10} of Aβ(1-28) [5,14,15]. Therefore, the electrostatic repulsive force between both residues should occur. In addition, the monomeric Aβ(1–40) interacted with the positively charged 1,2-dioleoyl-3-trimethyl ammonium propane (DOTAP) liposome at around pH 7, not with the negatively charged DMPG liposome [8]. However, Fig. 3B shows the clear interaction between Aβ(1–40) seeds and DMPG liposomes. The seeds with 100 nm in approximately length were then prepared (Fig. 4A). We observed the seeds suspension mixing with DMPG liposomes for 50 min. The association of seeds of Aβ(1–40) fibrils with DMPG liposome was definitely observed as shown in Fig. 4B. The elongated fibrils were not observed in this condition.

We then discuss the interaction between the seeds and liposome membranes in terms of structural feature of Aβ(1–40) fibrils previously reported [16]. Aβ(1–40) sequence is divided into the polar region (Asp^{1}-Lys^{28}), with both positive (Arg^{5}, His^{13}, His^{14}, Lys^{16}, Lys^{28}) and negative (Asp^{1}, Glu^{2}, Asp^{7}, Glu^{11}, Glu^{22}, Asp^{23}) charges, and the hydrophobic transmembrane regions (Gly^{29}-Val^{40}) [1]. Previous study shows that Arg^{5} and Lys^{16} are not required for Aβ-lipid interaction [11]. Among amino acid sequences for Aβ(1–40), Lys^{28} is used to form the salt-bridge with Asp^{23} within amyloid fibril structure while Lys^{16} faces into bulk [16]. Since the seeds prepared in advance were externally added to the liposome suspension, only a Lys^{16} can interact with negatively charged DMPG molecule. Therefore, the hydrophobic interface should expose into the bulk aqueous phase, followed by the interaction between the hydrophobic interfaces of seeds. This is considered to be suggested by Fig. 3B.

In order to clarify the contribution of the structure of seeds, the growth behavior of seeds and monomer of Aβ(1–40) was compared. Obviously, the growth of seeds over 80 min was observed as shown in Fig. 4E–H. Meanwhile, no spherulite was observed in the case of spontaneous growth of Aβ(1–40) monomer (Fig. 4I–L). The same was true for DMPA and DMPS liposomes (data not shown). From these observations, we hypothesized the possible mechanism of spherulite formation (Fig. 4Scheme). This process may behave as the liposome-mediated seed aggregation process. This is because the formation of hydrophobic environment is advantageous for the stabilization of hydrogen bonding in the fibril growth, as elucidated from previous report [17]. In the center of spherulite and at around, we observed no association of DMPG liposome with fibrils (Fig. 4C). In contrast, we could observe the region where fibrils bound to liposomes, at the edge of spherulites (Fig. 4D). The samples used in TIRFM observation were also

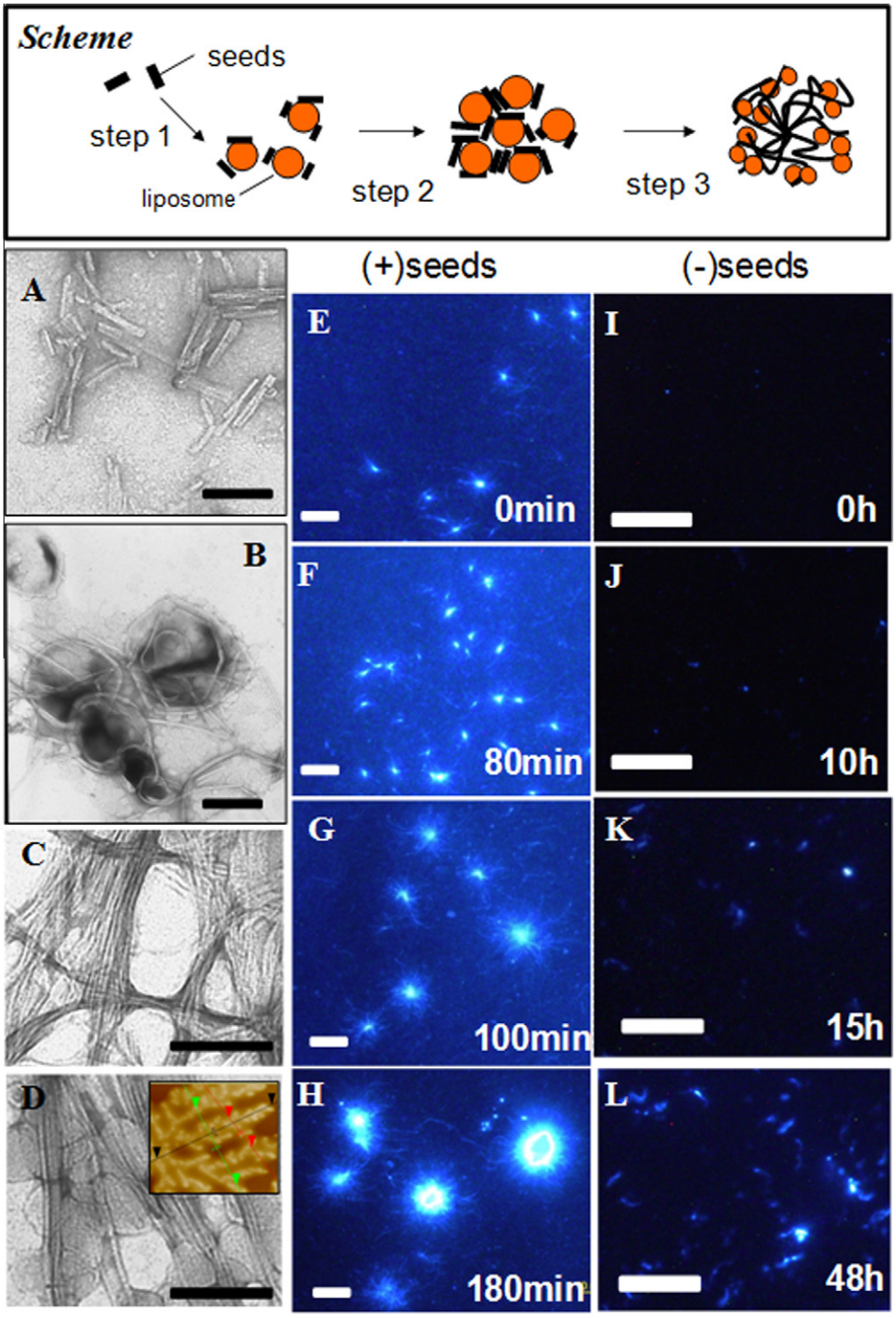

Fig. 4. Possible scheme on formation of spherulitic fibrillar aggregate and SEM images of (A) seeds of amyloid fibrils and (B) mixture of seeds/DMPG liposomes (80 min later). (C) TEM image of non-liposome region and (d) liposome region of grew fibrils from seeds/DMPG liposomes (180 min later) and its AFM image (insert in D). TIRFM images of the time-course of amyloid fibril formation of Aβ fibrils in (E–H) the presence and (I–L) the absence of seeds. Bars: (white)10 μm (black) 200 nm.

transferred onto mica stage for the atomic force microscopy (AFM) observation. The observed image implied the possibility of DMPG liposomes associating with fibrils (Insert in Fig. 4D), although spherulitic assemblies were partly broken during the transfer from the suspension to mica substrate. Similarly, the association of DMPA and DMPS liposomes with fibrils was also observed. Therefore, we can fairly conclude that the spherulitic structures were constructed by concerting the growth of seeds with the anionic liposome-induced aggregate of seeds.

In conclusion, we successfully demonstrated the reproducible modeling of the senile plaque formation of Aβ(1–40) under the physiological conditions. The advantage in the present method needed neither the substrates structured specifically by polymers [2] nor extremely preparation conditions [3]. This method is

considered to have great potential for application to experiments in the field of neuroscience and cell biology.

Acknowledgments

The authors are also grateful for Mr. M. Kawashima of the Gas Hydrate Analyzing System (Osaka Univ.) for his experimental assistant on SEM and AFM observations. A part of the present experiments was carried out by using a facility in the Research Center for Ultrahigh Voltage Electron Microscopy (Osaka University). This work was supported by Grant-in-Aid for Scientific Research from the Ministry of Education, Science, Sports, and Culture of Japan (Nos. 23656525 and 24686086) and partly, by a Cabinet Office NEXT program (No. GR066).

References

[1] M.P. Mattson, Pathways towards and away from Alzheimer's disease, Nature 430 (2004) 631–639.

[2] H. Yagi, T. Ban, K. Morigaki, H. Naiki, Y. Goto, Visualization and classification of amyloid β supramolecular assemblies, Biochemistry 46 (2007) 15009–15017.

[3] M.R.H. Krebs, C.E. MacPhee, A.F. Miller, I.E. Dunlop, C.M. Dobson, A.M. Donald, The formation of spherulites by amyloid fibrils of bovine insulin, Proc Natl. Acad. Sci. U. S. A. 101 (40) (2004) 14420–14424.

[4] M.R.H. Krebs, E.H.C. Bromley, S.S. Rogers, A.M. Donald, The mechanism of amyloid spherulite formation by bovine insulin, Biophys. J. 88 (3) (2005) 2013–2021.

[5] T. Ban, K. Morigaki, H. Yagi, T. Kawasaki, A. Kobayashi, S. Yuba, H. Naiki, Y. Goto, Real-time and single fibril observation of the formation of amyloid β spherulitic structures, J. Biol. Chem. 281 (44) (2006) 33677–33683.

[6] V. Koppaka, C. Paul, I.V.J. Murray, P.H. Axelsen, Early synergy between Aβ42 and oxidatively damaged membranes in promoting amyloid fibril formation by Aβ40, J. Biol. Chem. 278 (38) (2003) 36277–36284.

[7] S. Morita, Y. Hamano, R. Kuboi, Effect of fatty acids on interaction between liposome and amyloid β-peptide, Maku (Memb.) 32 (4) (2007) 215–220.

[8] K. Ikeda, K. Matsuzaki, Driving force of binding of amyloid β-protein to lipid bilayers, Biochem. Biophys. Res. Comm. 370 (2008) 525–529.

[9] R. Kuboi, T. Shimanouchi, M. Yoshimoto, H. Umakoshi, Detection of conformational change of protein under stress conditions, Sensors Mater. 16 (2004) 241–254.

[10] K. Matsuzaki, Physicochemical interactions of amyloid β-peptide with lipid bilayers, Biochim. Biophys. Acta 1768 (2007) 1935–1942.

[11] A. Chauhan, I. Ray, V.P.S. Chauhan, Interaction of amyloid beta-protein with anionic phospholipids: possible involvement of Lys28 and C-terminus aliphatic amino acids, Neurochem. Res. 25 (3) (2000) 423–429.

[12] H. Naiki, K. Nakakuki, First-order kinetic model of Alzheimer's β-amyloid fibril extension in vitro, Lab. Invest. 74 (2) (1996) 374–383.

[13] J.A. Kotarek, K.C. Johnson, M.A. Moss, Quartz crystal microbalance analysis of growth kinetics for aggregation intermediates of the amyloid β protein, Anal. Biochem. 378 (2008) 15–24.

[14] S. Zhang, J.P. Lee, Selectively 2H-labeled Glu/Asp: application to pK_a measurements in Aβ amyloid peptides, J. Pept. Res. 55 (2000) 1–6.

[15] K. Ma, E.L. Clancy, Y. Zhang, D.G. Ray, K. Wollenberg, M.G. Zagorski, Residue-specific pK_a measurements of the β-peptide and mechanism of pH-induced amyloid formation, J. Am. Chem. Soc. 121 (1999) 8698–8706.

[16] A.T. Petkova, Y. Ishii, J.J. Balbach, O.N. Antzutkin, R.D. Leapman, F. Delaglio, R. Tycko, A structural model for Alzheimer's β-amyloid fibrils based on experimental constraints from solid state NMR, Proc. Natl. Acad. Sci. U. S. A. 99 (26) (2002) 16742–16747.

[17] A. Fernandez, What factor drives the fibrillogenic association of β-sheets?, FEBS Lett 579 (2005) 6635–6640.